

References

1. A. K. Oppenheim, N. Manson, H. G. Wagner, *Amer. Inst. Aeronaut. Astronaut. J.* **1**, 2243 (1963); D. R. White, *Phys. Fluids* **4**, 465 (1961); R. E. Duff, *ibid.*, p. 1427.
2. Y. H. Denisov and Y. K. Troshin, *Dokl. Akad. Nauk SSSR* **125**, 110 (1959) [transl. *Phys. Chem. Sect.* **125**, 217 (1960)]; *Zh. Tekh. Fiz.* **30**, 450 (1960); K. I. Shtselkin, *Dokl. Akad. Nauk SSSR* **47**, 501 (1945).
3. A. W. Campbell, T. E. Holland, M. E. Malin, T. P. Cotter, *Nature* **178**, 38 (1956); H. Dean Mallory, *J. Appl. Phys.* **38**, No. 13, 5302 (1967).
4. H. Dean Mallory and R. A. Plauson, *Nature* **199**, 18 (1963).
5. B. B. Dunne, *Phys. Fluids* **4**, 918 (1961).
6. ———, *ibid.*, p. 1565.
7. R. I. Soloukhin, *Shock Waves and Detonations in Gases* (Mono, Baltimore, 1966), p. 138.

6 October 1969; revised 10 December 1969 ■

Electron Population Parameters from Least-Squares Refinement of X-ray Diffraction Data

Abstract. A least-squares refinement of x-ray diffraction data has been developed in which the parameters are the populations of atomic orbital products describing the molecular electron density distribution. The procedure is applied to α -oxalic acid dihydrate and cyanuric acid. Complementary structural information obtained by neutron diffraction has been used. In the absence of complementary information, the method allows simultaneous determination of structural and charge-density parameters. There is an indication of a migration of charge from the p_π to the p_σ orbitals in both molecules.

A number of recent studies have shown that information on the electron distribution in molecules can be obtained from diffraction data (1-5). The redistribution of electrons upon the formation of a molecule has been illustrated through Fourier difference maps, obtained either through a combination of x-ray and neutron diffraction data (2, 3), or by use of parameters from high-order x-ray refinements (4, 5).

Such Fourier maps are illustrative but do not provide quantitative information for direct comparison with theoretical calculations. An alternative procedure, outlined here, is the determination by least-squares refinement of x-ray diffraction data of parameters describing the electron density.

If the molecular orbitals ψ_i are mu-

tually orthogonal linear combinations of atomic orbitals φ_μ , with coefficients $C_{i\mu}$, the one-electron density function ρ is described by a summation of orbital products $\varphi_\mu\varphi_\nu$, each multiplied by an appropriate population coefficient $P_{\mu\nu}$:

$$\psi_i = \sum_{\mu} C_{i\mu} \varphi_{\mu} \quad (1)$$

$$\rho = 2 \sum_{\mu} \sum_{\nu} \sum_i^{occ} C_{i\mu} C_{i\nu} \varphi_{\mu} \varphi_{\nu} \equiv \sum_{\mu} \sum_{\nu} P_{\mu\nu} \varphi_{\mu} \varphi_{\nu} \quad (2)$$

The evaluation of the x-ray scattering of the density described by the orbital products $\varphi_\mu\varphi_\nu$ is facilitated considerably when the atomic orbitals are expressed as linear combinations of

Gaussian type orbitals. The appropriate expressions and constants have been given by Stewart (6).

The x-ray observations give information on the electron density time-averaged over the vibrations of the molecule in the crystal. In the present treatment we allow for thermal motion by assuming that each one-center orbital product experiences the same motion as the nucleus on which it is centered, whereas the two-center orbital products are assumed to vibrate with a mean-square amplitude which is the average of the amplitudes of the two centers.

We have tested two different models. In the first, a one-center model, all cross products between orbitals on different atoms are neglected. In the second model, a limited multicenter model, cross products between adjacent covalently bonded atoms in the molecule are included. In the calculations reported here a minimum Hartree-Fock (HF) basis set of $1s$, $2s$, $2p_x$, $2p_y$, and $2p_z$ orbitals for carbon, nitrogen, and oxygen atoms and $1s$ orbitals for hydrogen atoms is used. The method is by no means limited, however, to a Hartree-Fock basis set. Indeed, similar calculations with Slater-type orbitals have been completed.

The $1s$ electrons of the C, N, and O atoms are assumed to be unperturbed by bonding, thus eliminating $1s^2$ population coefficients as parameters in the least-squares refinement. Short-range migrations of charge near the nucleus are not observable with this technique, because of the limited resolution of the x-ray diffraction data.

Early experience indicated a large correlation between the $2s^2$ population and a spherical sum of the p_x^2 , p_y^2 , and p_z^2 orbital products, resulting from the almost equal radial dependences of the time-averaged $2s$ and $2p$ orbitals (6). The $2s^2$ population was therefore fixed at an arbitrary value in subsequent calculations. A full description of the asphericity of the valence electrons was obtained by variation of the population of the p_x^2 , p_y^2 , and p_z^2 orbital products. Hence nine one-center population parameters are included for each heavy atom in a general crystallographic position; they are the coefficients $P_{\mu\nu}$ listed in Tables 1 and 2. Symmetry requirements reduce the number of parameters for atoms in special positions.

Using positional and thermal parameters obtained by neutron diffraction, we applied the one-center model to the x-ray diffraction data on α -oxalic acid dihydrate (3) and cyanuric acid (4).

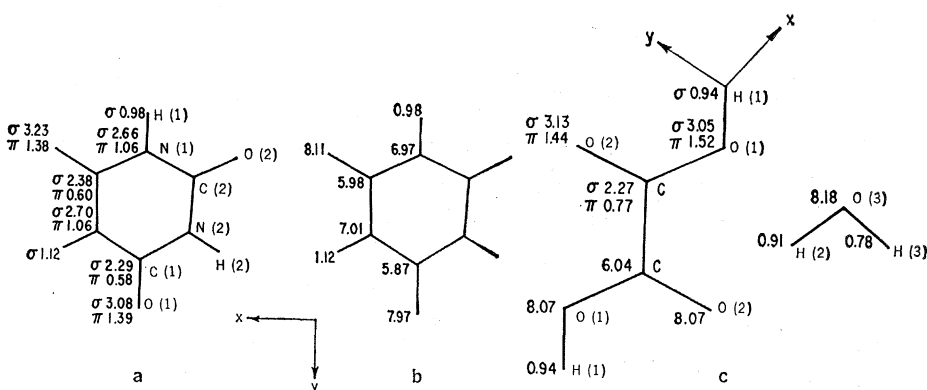


Fig. 1. Experimental charge distributions in cyanuric acid (a and b), and in α -oxalic acid dihydrate (c) obtained with the Hartree-Fock basis set. Figure 1a and the upper half of the oxalic acid molecule in Fig. 1c show the division into p_σ and p_π populations, whereas the total charge distribution is given in Fig. 1b and the remaining part of Fig. 1c. The two halves of the oxalic acid molecule and the two halves of the cyanuric acid molecule are related by crystallographic symmetry elements. The $2s^2$ populations of the C, N, and O atoms are set at 1.0, 1.25, and 1.50 electrons, respectively.

In this case the least-squares equations are linear, and one cycle leads to convergence. In the refinement the total number of electrons is constrained so that the crystal remains neutral. Results are given in Tables 1 and 2 and Fig. 1. The model produces an appreciable reduction in the indices of agreement and satisfying agreement between the population parameters of chemically equivalent atoms in cyanuric acid. Although the one-center model excludes the overlap-density terms that are included in the multicenter treatments, it allows density to be built up in bond regions through the population of the $2s2p$ and $2p_i2p_j$ cross terms. For example, when the $2sp_x$ orbital product has a positive population, density is shifted from points with negative x coordinates to points with positive x coordinates, whereas the $p_x p_x$ function is positive in two quadrants and negative in the others.

In the multicenter models with the basis set of orbitals described above, the electron density in a bond is represented by $4 \times 4 = 16$ orbital products. For a bond AB parallel to the y -axis, the electron distributions described by $2p_x(A)2p_x(B)$ and $2p_x(A)2p_z(B)$ are equivalent. This implies that only the sum of the two population parameters can be determined from diffraction data.

Large correlations are often found between the remaining 15 bond parameters and one-center terms such as $2sp_x$, which can simulate the overlap density. This sometimes leads to ill-conditioning of the least-squares matrix. Although a 117-parameter set, which includes 15 terms for each of the covalent bonds, produces good convergence for cyanuric acid, the parameter correlation introduces a certain arbitrariness in the results. This arbitrariness may be eliminated by selection of a smaller set of parameters according to chemical or mathematical criteria, or both.

In calculating the electron distribution for the two molecules, we have not used *ab initio* self-consistent-field methods, but, using the INDO (intermediate neglect of differential overlap) method (7), we have undertaken approximate calculations for all the valence electrons. The theoretical values for cyanuric acid are compared with experimental results obtained with Hartree-Fock and optimized Slater (8) basis sets in Table 3. The most striking discrepancy is the small observed population of the p_{π^2} orbital products on the N and C atoms, and to some extent

Table 1. One-center population coefficients of Hartree-Fock orbital products for cyanuric acid at 100°K*. Numbers in parentheses are estimated standard deviations in the last digit. Parameters were not refined if no standard deviation is indicated. The z -axis is perpendicular to the molecular plane. The direction of the x - and y -axes and the numbering of the atoms are indicated in Fig. 1.

Orbital product	C(2)	C(1)	N(2)	N(1)	O(2)	O(1)	H(2)	H(1)
$1s^2$	2.0	2.0	2.0	2.0	2.0	2.0	1.12(5)	0.98(7)
$2s^2$	1.0	1.0	1.25	1.25	1.50	1.50		
p_x^2	1.33(5)	1.08(7)	1.37(4)	1.24(5)	1.63(3)	1.53(4)		
p_y^2	1.05(5)	1.21(7)	1.33(4)	1.42(5)	1.60(3)	1.55(4)		
p_z^2	0.60(4)	0.58(6)	1.06(4)	1.06(5)	1.38(3)	1.39(4)		
$p_x p_y$	-0.07(7)	0	0.04(5)	0	-0.07(5)	0		
$p_x p_z$	0.08(6)	-0.08(9)	-0.02(5)	-0.10(4)	0.01(5)	0.07(8)		
$p_y p_z$	-0.01(6)	0	0.10(5)	0	-0.09(5)	0		
sp_x	0.07(5)	0	0.10(4)	0	0.28(3)	0		
sp_y	-0.04(6)	-0.10(8)	-0.01(4)	-0.09(5)	-0.10(3)	0.13(5)		
sp_z	0.02(5)	0	0.01(4)	0	0.07(3)	0		
Total atomic population (electrons)								
	5.98	5.87	7.01	6.97	8.11	7.97	1.12	0.98
* $R = \frac{\sum F_o - F_c }{\sum F_o}$ $R_w = \left\{ \frac{\sum w F_o - F_c ^2}{\sum w F_o^2} \right\}^{1/2}$								
$R : 0.042 \rightarrow 0.040$ $R_w : 0.047 \rightarrow 0.039$								

The quantities R and R_w are the indices of agreement between the observed and calculated structure factors (F_o and F_c , respectively); w is the experimental weight assigned to each of the structure factors. The values on the left of the arrows correspond to spherical neutral atoms and refined neutron parameters. The reduction in R is obtained by refining only the population parameters. If the scale factor is also adjusted, R and R_w reduce to 0.038 and 0.036, respectively; the corresponding change in population parameters is small.

Table 2. One-center population coefficients for α -oxalic acid dihydrate*. For explanation of details, see Table 1.

Orbital product	C	O(1)	O(2)	O(3)	H(1)	H(2)	H(3)
$1s^2$	2.0	2.0	2.0	2.0	0.94(3)	0.91(3)	0.78(4)
$2s^2$	1.0	1.50	1.50	1.50			
p_x^2	1.07(4)	1.51(4)	1.51(3)	1.52(3)			
p_y^2	1.20(6)	1.54(4)	1.62(5)	1.41(4)			
p_z^2	0.77(4)	1.52(4)	1.44(4)	1.75(4)			
$p_x p_y$	0.13(7)	-0.14(7)	0.01(6)	-0.21(6)			
$p_x p_z$	-0.08(7)	-0.07(7)	-0.18(6)	-0.10(6)			
$p_y p_z$	-0.23(7)	-0.05(7)	-0.19(7)	-0.25(7)			
sp_x	-0.12(4)	-0.10(3)	0.00(3)	0.00(3)			
sp_y	0.01(5)	0.02(3)	0.04(4)	-0.06(3)			
sp_z	0.06(4)	-0.02(3)	-0.01(3)	0.14			
Total atomic population (electrons)							
	6.04	8.07	8.07	8.18	0.94	0.91	0.78

* $R : 0.047 \rightarrow 0.031$; $R_w : 0.053 \rightarrow 0.029$.

Table 3. Distribution of electrons between σ - and π -orbitals in cyanuric acid. Experimental population of $2s$ orbitals has been adjusted to the theoretical values. Compensating changes have been made in the spherical average of the p_{π^2} and p_{σ^2} products. The two entries for each of the experimental quantities refer to the two crystallographically independent atoms.

Method	Electron population			Net charge
	s^*	σ	π	
Carbon				
Observed HF basis set	1.00, 1.00	2.38, 2.29	0.60, 0.58	+0.02, +0.13
Observed Slater basis set	1.00, 1.00	2.20, 2.14	0.55, 0.59	+0.25, +0.27
Calculated INDO	1.00	1.66	0.80	+0.54
Nitrogen				
Observed HF basis set	1.21, 1.21	2.73, 2.69	1.07, 1.07	-0.01, +0.03
Observed Slater basis set	1.21, 1.21	2.90, 2.80	1.23, 1.22	-0.34, -0.23
Calculated INDO	1.21	2.35	1.74	-0.30
Oxygen				
Observed HF basis set	1.78, 1.78	3.04, 2.89	1.29, 1.30	-0.11, +0.03
Observed Slater basis set	1.78, 1.78	2.90, 2.92	1.30, 1.33	+0.02, -0.03
Calculated INDO	1.78	3.18	1.46	-0.42
Hydrogen				
Observed HF basis set	1.14, 0.98			-0.14, +0.02
Observed Slater basis set	0.95, 0.89			+0.05, +0.11
Calculated INDO	0.83			+0.17

* For C, N, and O, s represents the $2s$ orbital; for H, s represents the $1s$ orbital.

also on the O atom. Approximate balance of charge is retained by an increase in the populations of the σ -orbitals. This effect, which is also observed in oxalic acid, would imply that in the crystal there is more concentration of charge in the molecular plane than the approximate calculation on the isolated molecule would predict. Net atomic charges are generally smaller than the calculated values, although the results obtained with the optimized Slater basis set are closer to the theoretical values for the C, N, and H atoms.

P. COPPENS, L. CSONKA
T. V. WILLOUGHBY

Chemistry Department, State University
of New York, Buffalo 14214

References and Notes

1. A. M. O'Connell, A. I. M. Rae, E. N. Maslen, *Acta Crystallogr.* **21**, 208 (1966); B. Dawson, *Proc. Roy. Soc. London Ser. A* **298**, 264 (1967).
2. P. Coppens, *Science* **158**, 1577 (1967).
3. ———, T. M. Sabine, R. G. Delaplane, J. A. Ibers, *Acta Crystallogr.* **B25**, 2451 (1969).
4. G. C. Verschoor, thesis, University of Groningen, Holland (1967).
5. R. F. Stewart and L. H. Jensen, *Z. Kristallogr.* **128**, 133 (1969).
6. R. F. Stewart, *J. Chem. Phys.* **50**, 2485 (1969); *ibid.* **51**, 4569 (1969).
7. J. A. Pople, D. L. Beveridge, P. A. Dobosh, *ibid.* **47**, 2026 (1967).
8. W. J. Hehre, R. F. Stewart, J. A. Pople, *ibid.* **51**, 2657 (1969).
9. We thank Dr. G. C. Verschoor and A. Vos for making the x-ray data on cyanuric acid available and Drs. R. G. Delaplane and J. A. Ibers for the x-ray data on α -oxalic acid dihydrate. We are grateful to Dr. J. W. McIver for use of his INDO program. Supported by the National Science Foundation under grant No. GP-10073 and the Petroleum Research Fund under grant No. 4518-AC5.

7 October 1969; revised 1 December 1969 ■

Crustal Plates in the Central Atlantic

Abstract. Various people have proposed that North and South America are a part of a gigantic crustal plate within which little differential movement is taking place. Considerations of the size of this postulated plate and the pattern of seismicity around the Caribbean indicate that it is in fact two plates, separated in the region between the Lesser Antilles and the Mid-Atlantic Ridge. Many of the offsets of the Mid-Atlantic Ridge opposite the Caribbean are the result of differential spreading rates and the westward continuations of the fracture zones extending from these offsets are active left-lateral faults.

In the consideration of data regarding a portion of a fracture zone beyond a ridge offset Fox *et al.* (1) adhere to the related concepts of the ridge-ridge transform fault (2) and plate tectonism (3-5). According to these ideas the present configuration of the ridge preserves the shape of the original opening of the ocean basin, crust moves away from the ridge in gigantic unsheread plates, ridge offsets are transform faults that terminate at the ridge, and the topographic expression of the fracture zones outside of the ridge offsets results from the positive elevation of the side closest to the ridge.

Our work (6) has led us to an alternate explanation for the origin of some fracture zones. We began in an attempt to explain the structural and seismic asymmetry between the north and south boundaries of the Caribbean Sea. We concluded that left-lateral shear in the Atlantic to the east of the Caribbean (Fig. 1) was necessary to explain the relative lack, both of earthquakes, and also of evidence for strike-slip motion on the south boundary of the Caribbean Sea. This led us to question the assumption (3-5) that both North and South America together with the Western Atlantic act as a single plate.

We were initially impressed by the great size and extremely irregular shape of this plate with its narrow section between the Mid-Atlantic Ridge and the Caribbean. As Morgan points out (4), it is impossible to tell with his approach whether the Americas are parts of one or two plates. This is because the evidence which he obtained from the strikes of offsets of the Mid-Atlantic

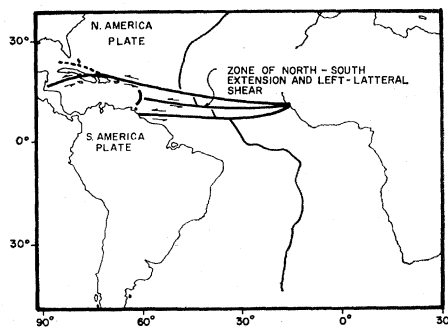


Fig. 1. After Funnell and Smith (1968). The Mid-Atlantic Ridge is shown schematically. Geometric reconstruction of the Atlantic indicates that North America has moved faster and slightly to the north relative to South America's movement away from Africa. The result of the relative movement between these plates has been the formation of a zone of north-south extension and left-lateral shear.

Ridge gives a pole of rotation that is poorly defined with regard to latitude. It is equally possible to choose two poles of rotation, the one for North America and Africa lying to the north of the one for South America and Africa.

The evidence for a single pole from the variation of spreading rate with position on the ridge, used by Morgan, is equally inconclusive. The data points are clustered between 22° and 32°N and 24° and 44°S. The data are just as well explained as a result of North and South America acting as parts of different plates rotating away from Africa about different poles of rotation at different speeds.

Based on the geometrical reconstruction of the Atlantic (7), Funnell and Smith (8) came to the conclusion that the Caribbean region was formed because North America rotated away from Africa faster and with a more northerly component than South America. The Caribbean and that portion of the Atlantic to the east of the Lesser Antilles would accordingly be a region of north-south extension and left-lateral shear.

This region is the site of numerous offsets of the Mid-Atlantic Ridge. Based on the position of these segments the sense of shear on these offsets appears to be left-lateral. However, judging from first motion studies on the offsets the sense of shear is right-lateral (9). This paradoxical situation is resolved by consideration of the interaction of fracture zone faults and migrating ridges. The Mid-Atlantic Ridge must migrate westward from Africa because of the lack of a marginal trench system about this ridge-ringed continent (10). As a result of a faster spreading rate the migration has been more rapid to the north of latitude 5°N (Fig. 1). Fracture zone faults offsetting the ridge are the result of this incremental variation in ridge migration rate.

Both ridge segments are migrating to the left in order to accommodate new crust formed by spreading (Fig. 2). The northern segment migrates faster as a result of its greater spreading rate. This shears and offsets the ridge. Shear is no longer active on the part of the fracture zone between the ridge and the fixed continental margin; however, the pattern of magnetic anomalies will record the progressive left-lateral offsetting of the ridge on this dead fault. Between the portions of ridge crest, the north side of the fracture zone is fixed relative to the conti-